ACS Catalysis

Research Article

pubs.acs.org/acscatalysis

Unraveling the Crucial Role of Metal-Free Catalysis in Borazine and Polyborazylene Formation in Transition-Metal-Catalyzed Ammonia–Borane Dehydrogenation

Sourav Bhunya,[†] Paul M. Zimmerman,[‡] and Ankan Paul*[,†]

[†]Raman Centre for Atomic, Molecular and Optical Science, Indian Association for the Cultivation of Science, Kolkata 700 032, India

[‡]Department of Chemistry, University of Michigan, 930 North University Avenue, Ann Arbor, Michigan 48109, United States

Supporting Information

ABSTRACT: Though the recent scientific literature is rife with experimental and theoretical studies on transition-metal (TM)-catalyzed dehydrogenation of ammonia–borane (NH_3·BH_3) due to its relevance in chemical hydrogen storage, the mechanistic knowledge is mostly restricted to the formation of aminoborane (NH_2BH_2) after 1 equiv of H_2 removal from NH_3·BH_3. Unfortunately, the chemistry behind the formation of borazine and polyborazylene, which happens only after more than 1 equiv of H_2 is released from ammonia–borane in these TM-catalyzed homogeneous reactions, largely remains unknown. In this work we use density functional theory to unravel the curious function of "free NH_2BH_2". Initially, free NH_2BH_2 molecules form oligomers such as cyclotriborazane and *B*-(cyclodiborazanyl)aminoborohydride. We show that, through a web of concerted proton and hydride transfer based dehydrogenations of oligomeric intermediates, cycloaddition reactions, and hydroboration steps facilitated by NH_2BH_2, the development of the polyborazylene framework occurs. The rate-determining free energy barrier for the formation of a polyborazylene template is predicted to be 25.7 kcal/mol at the M05-2X(SMD)/6-31++G(d,p)//M05-2X/6-31++G(d,p) level of theory. The dehydrogenation of BN oligomeric intermediates by NH_2BH_2 yields NH_3·BH_3, suggesting for certain catalytic systems that the role of the TM catalyst is limited to the dehydrogenation of NH_3·BH_3 to maintain optimal amounts of free NH_2BH_2 in the reaction medium to enable polyborazylene formation. TM catalysts that fail to produce borazine and polyborazylene falter because they rapidly consume NH_2BH_2 in TM-catalyzed polyaminoborane formation, thus preventing the chain of events triggered by NH_2BH_2.

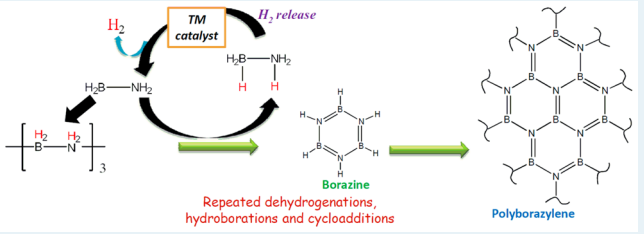

KEYWORDS: *ammonia–borane, chemical hydrogen storage, transition metal catalyst, redistribution, second and third equivalent hydrogens, metal-free catalysis*

INTRODUCTION

Ammonia–borane (NH_3·BH_3, **1**) has garnered significant interest as a plausible chemical hydrogen storage material due to its high volumetric and gravimetric hydrogen content.[1] H_2 can be released from **1** by catalysts that exploit the protic nature of the N–H hydrogen and the hydridic nature of the B–H hydrogen of **1**. A recent surge in the development of catalysts, both homogeneous and heterogeneous catalysts, for releasing H_2 from the available 3 equiv per molecule of **1** has been witnessed.[2,3] Among these, the homogeneous TM-containing organometallic catalysts can be broadly divided into two classes: (a) type I catalysts such as Brookhart's Ir(POCOP)H_2,[2a−c] Fagnou's ruthenium phosphino-amine complexes,[2d] Schneider's Ru(PNP)(H)(PMe_3) (PNP = HN($CH_2CH_2PiPr_2$)$_2$),[2e] Weller's [Ir(PCy_3)$_2$(H)$_2$(H_2)$_2$][$BArF_4$],[2f] and osmium dihydride complexes[2g] which are capable of extracting 1 equiv of H_2 from **1** and (b) type II catalysts such as Baker's Ni(NHC)$_2$,[2h] Shvo's catalyst,[2i] William's ruthenium bis(pyridyl)borate complex,[2j] and Guan's iron bis(phosphonite) complexes,[2k] which are capable of releasing more than 1 equiv of H_2. While type I catalysts lead to the formation of polyaminoborane,[2a−g] type II catalysts produce borazine and polyborazylene $(BNH)_x$[2h−k] as the main dehydropolymerized BN material. However, whether a homogeneous transition-metal catalyst would behave as a type I or type II catalyst is also dependent on experimental conditions. For instance, the Brookhart catalyst can behave as a type I catalyst at room temperature and also show traits of a type II catalyst at elevated temperatures of or around 60 °C with respect to dehydrogenation of **1**.[4]

The spurt in experimental activity in this area has aroused curiosity regarding the intrinsic mechanistic principles which control these catalytic processes.[3] The vast body of related theoretical work has largely been devoted to deciphering the working principles of extraction of 1 equiv of H_2 from **1** to generate aminoborane (NH_2BH_2, **2**) by several transition-metal catalysts.[5] However, a clear theoretical understanding of

Received: December 31, 2014
Revised: March 28, 2015
Published: April 15, 2015

DOI: 10.1021/cs502129m
ACS Catal. 2015, 5, 3478−3493

Scheme 1. Intermediates Isolated before Borazine Formation during the Thermal Dehydrogenation of Ammonia–Borane (1) by Autrey and Co-Workers[6d] using ^{11}B and ^{15}N NMR Spectroscopy

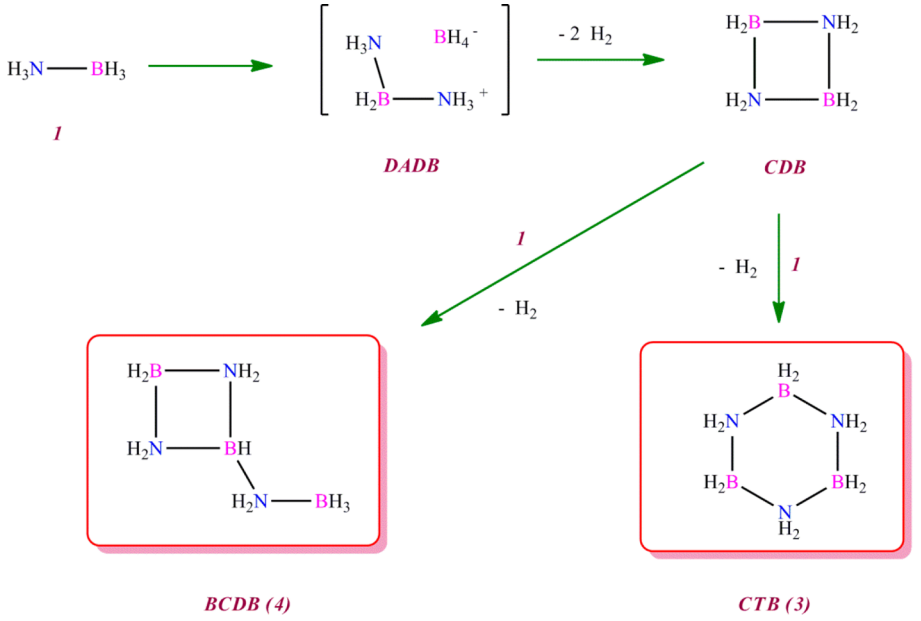

reaction pathways leading to formation of borazine and polyborazylene by catalyzed and uncatalyzed processes does not exist. Hence, the underpinnings of catalyst design for extracting higher equivalents of H_2 from **1** remains nebulous. One way to understand the chemistry at play is through identification of the intermediates generated during these catalytic processes. Using ^{11}B NMR studies, several experimental groups have reported that a cyclic trimer of NH_2BH_2, cyclotriborazane (**CTB**, **3**), is formed in cases where more than 1 equiv of H_2 is extracted from **1**, both in TM-catalyzed reactions[2h,6a−c] and in uncatalyzed dehydrocoupling of **1**[6d] (see Scheme 1). Along with **3**, other cyclic oligomers such as cyclodiborazane (**CDB**) and *B*-(cyclodiborazanyl)-aminoborohydride (**BCDB**, **4**) have also been identified before formation of borazine ($B_3N_3H_6$, **5**) (see Scheme 1).[6] Hence, one may infer from these experimental findings that catalysts (type II) which release more than 1 equiv of H_2 from **1** do so by dehydrogenating the oligomers of **2**. Theoretical studies have been able to rationalize the formation of most of the oligomers of **2**.[7] The perplexing question is why type II catalysts succeed and type I catalysts fail in extracting more than 1 equiv of H_2 from **1**. Intriguingly, type I catalysts generally produce insoluble linear polyaminoborane as the dehydrogenation byproduct,[2a−g] which is usually not observed for dehydrogenation reactions of **1** by type II catalysts.[2h−k]

To understand the chain of events which leads to oligomer formation in dehydrocoupling reactions of **1**, Baker and co-workers devised an elegant technique based on chemical entrapment of NH_2BH_2 (**2**) using cyclohexene.[4] They suggested that "free NH_2BH_2" is not released in the dehydrogenation reactions where the hydroboration product (Cy_2BNH_2) is not observed.[4] Interestingly, this technique when applied to type I catalyzed dehydrogenations of **1** suggests that free NH_2BH_2 may not be formed (see Scheme 2). Our recent theoretical studies indicate that "free NH_2BH_2" is not entrapped as Cy_2BNH_2 in cases of type I catalysts such as the Ir[POCOP]H_2 and ruthenium catalysts, as the NH_2BH_2 released in the reaction medium is rapidly consumed by the

Scheme 2. Two Different Classes of Transition-Metal Catalysts Used for Dehydrogenation of Ammonia–Borane (1) on the Basis of the Chemical Entrapment Technique of Baker and Co-Workers[4]

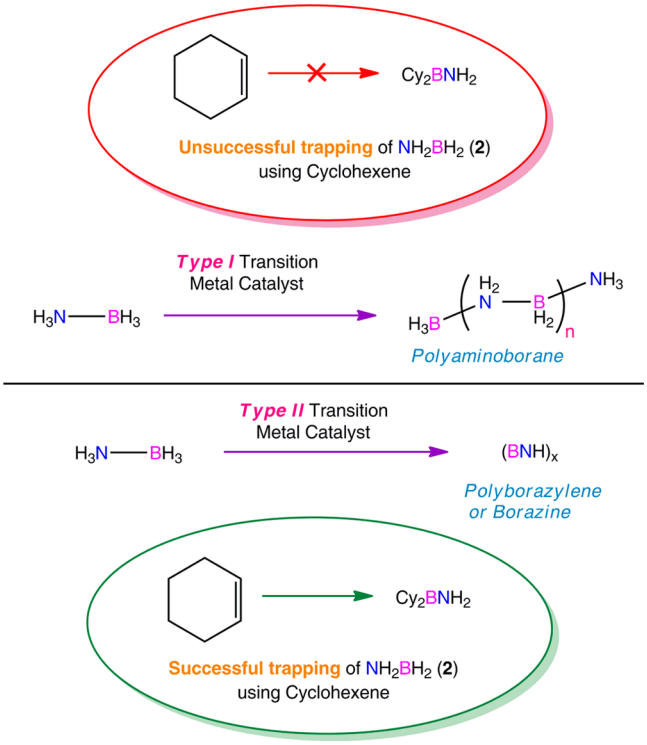

metal-assisted polyaminoborane formation reaction.[8] Our in-depth theoretical study revealed that Ir(POCOP)H_2 forms an in situ nucleophile by binding a NH_2BH_2 unit, which in turn acts as a chain initiation template for polyaminoborane formation (see Scheme 3).[8] Alternatively, for type II catalyzed dehydrogenation of **1**, free NH_2BH_2 is entrapped using excess cyclohexene (see Scheme 2).[4]

DOI: 10.1021/cs502129m
ACS Catal. 2015, 5, 3478−3493

Scheme 3. Reaction Pathways Leading to Polyaminoborane Formation by Ir(POCOP)H_2 As Shown by Paul and Co-Workers[8]

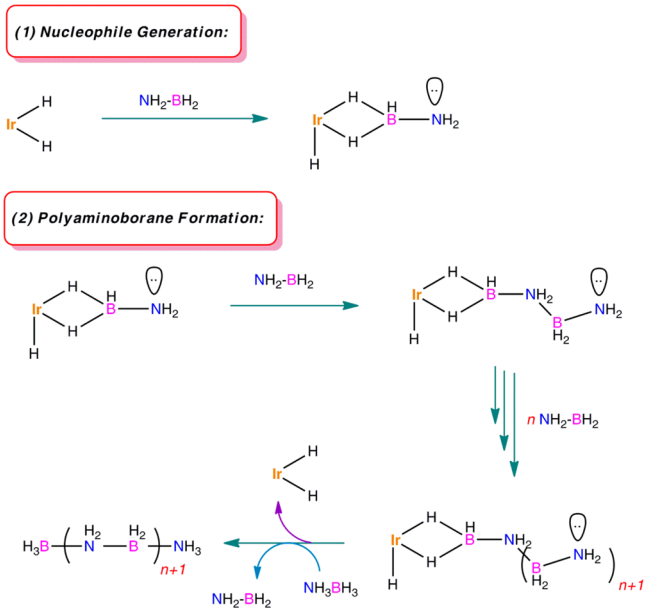

Another common trait in these reactions is that borazine and polyborazylene are usually produced around 60−70 °C.[2i−k] These features indicate that there may be an underlying commonality in the mechanism of removal of the second and third equivalents of H_2 by most type II catalysts. We surmised that the presence of "free NH_2BH_2" in the reaction media of type II catalyzed dehydrogenation reactions of **1** and the ability of these catalysts to exude more than 1 equiv of H_2 are interconnected. Moreover, the absence of "free NH_2BH_2" in dehydrogenation reactions of **1** by type I catalysts plausibly indicates the involvement of "free NH_2BH_2" in facilitating borazine and polyborazylene formation. Herein we report computational investigations which show that dehydrogenation reactions of **3** and **4** are triggered by NH_2BH_2. Dehydrogenation and further cycloaddition and hydroboration reactions through NH_2BH_2 are crucial for borazine and polyborazylene formation. NH_2BH_2 essentially plays the role of a catalyst in redistributing hydrogen from oligomers, which results in the formation of borazine and polyborazylene.

It is well documented, both theoretically and experimentally, that **2** and other aminoboranes can dehydrogenate amine−boranes and hydrogenated BN nanotubes through concerted proton and hydride abstraction, resulting in formation of the corresponding amine−borane.[7a,9] Zimmerman and co-workers[7a] showed theoretically that proton and hydride transfer between NH_2BH_2 and $NH_3{\cdot}BH_3$ happens through a low barrier route (see Scheme 4a). Experimentally it has been shown by Manners and co-workers that metal-free hydrogen transfer (both proton and hydride movement) takes place between a monomeric aminoborane, $NiPr_2BH_2$, and $NH_3{\cdot}BH_3$[9a,b] (see Scheme 4b). Additionally, theoretical calculations from our group suggested that hydrogenated BN nanotubes can be dehydrogenated by an aminoborane using the same principle (see Scheme 4c).[9c] Furthermore, we have shown that the protic and hydridic character is even retained on the hydrogen of a hydrogenated BN nanotube and can be exploited to release H_2.[9c] Hence, it can be expected that the hydrogen on oligomers

Scheme 4. Concerted Proton Hydride Transfer between Amine−Borane and Aminoborane: (a) Theoretically Proposed by Zimmerman and Co-Workers;[7a] (b) Experimentally Demonstrated by Manners and Co-Workers;[9a,b] (c) Theoretically Proposed by Paul and Co-Workers[9c]

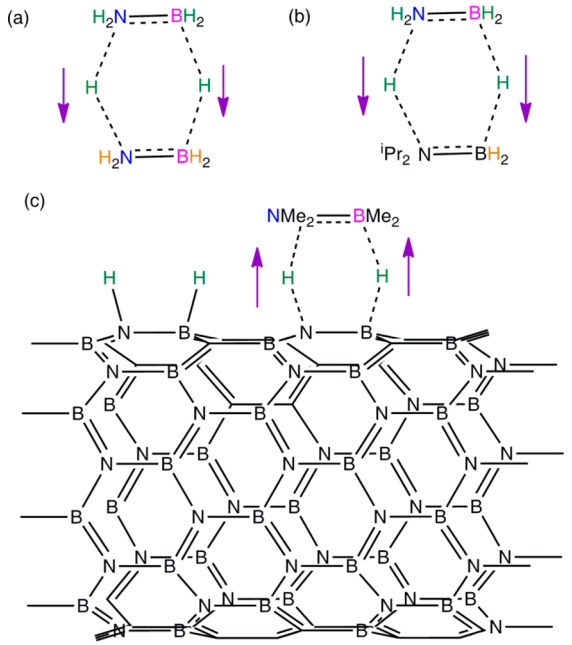

[a]The direction of dihydrogen transfer is shown by purple arrows.

of NH_2BH_2 would also retain the protic and the hydridic character. Evidently, this unique characteristic would render these oligomeric species vulnerable to dehydrogenation by bifunctional agents. One can thus fathom a pathway where **2** can dehydrogenate oligomers such as **CTB** and **BCDB** to yield borazine through repeated concerted dehydrogenations, converting **2** into **1**. This cycle can operate catalytically in the presence of a TM catalyst, which can dehydrogenate **1** to regenerate **2**, and **2** in turn would carry on the dehydrogenation of BN oligomers. Such a cycle suggests the TM catalyst abstracts hydrogen from **1** but not from the oligomers produced along the route. Using density functional techniques, we have investigated this possibility and provide crucial evidence that this is indeed a viable mechanism. Furthermore, we have investigated the barriers for hydrogen abstraction from oligomers of aminoborane by a Ir-based popular transition-metal catalyst,[2a] an N-heterocyclic carbene,[2h,5b] and an imine.[6b] On the basis of the findings from these investigations we present a plausible mechanistic picture of catalysis with an active role from aminoborane, which is at play for TM catalyzed higher equivalents of H_2 release from ammonia−borane.

COMPUTATIONAL DETAILS

All calculations were conducted using density functional theory (DFT) within the Gaussian09 suite of programs.[10] Intermediates and transition states were identified through geometry optimization followed by computing Hessians of energy with respect to nuclear coordinates. Intermediates were characterized by the presence of all real harmonic frequencies. Transition states were identified by the presence of a single imaginary frequency and by checking if the imaginary mode corresponds to the anticipated reaction coordinate. Moreover,

DOI: 10.1021/cs502129m
ACS Catal. 2015, 5, 3478−3493

Scheme 5. All Possible Routes for Formation of Borazine (5) from CTB (3)[a]

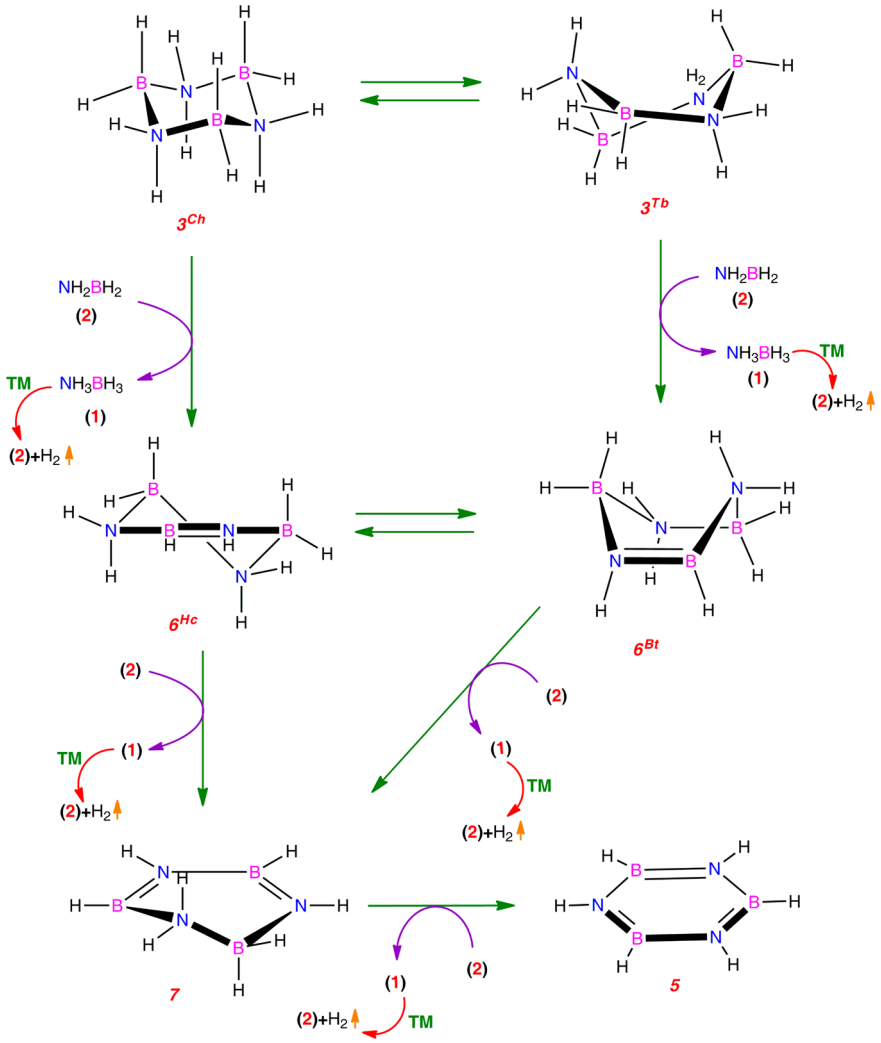

[a]TM = transition-metal-catalyzed irreversible release of H_2 from **1** and concomitant regeneration of **2**.

we have conducted intrinsic reaction coordinate (IRC) studies to ensure that each transition state is connected with the respective reactant and product. We have used the M05-2X[11] functional to obtain the gas phase optimized geometries of intermediates and transition states in conjunction with the 6-31++g(d,p) basis set. We have accounted for the effect of solvent in energy along the reaction pathways by performing single-point calculations within the SMD[12] solvent model and tetrahydrofuran (THF) (ε = 7.4257) as solvent using M05-2X with the 6-31++g(d,p) basis set on each atom. Determining exact entropies in the solution phase is still a challenge. Wertz and co-workers[13a] have developed an approach to resolve this problem. From experiments they have shown that solutes lose approximately 50−60% of their gas phase entropies. Therefore, solvent phase free energies were estimated for 298 K and 1 atmospheric pressure by using the solvent phase entropies, which were in turn obtained by empirically scaling gas-phase entropies by a factor of 0.5. This empirical approach for obtaining solvent phase entropic corrections from ideal gas model based computed gas phase entropies has been widely used in other density functional studies of reaction mechanisms.[13b−h] All thermodynamic free energy corrections were obtained at the M05-2X level of theory. Rate-determining barriers were further checked with M06-2X,[14] ωB97X-D,[15] M06-L,[16] and B97-D[17] functionals using the same methodology as was adopted for the M05-2X functional. In the following text we discuss the relevant stabilities, reaction energies, and reaction barriers in terms of solvent phase free energies at the M05-2X level of theory, if not mentioned otherwise. We have also checked the rate-determining barriers using second-order Møller−Plesset perturbation theory (MP2)[18] in conjunction with cc-pVTZ basis sets by conducting gas phase optimizations, followed by computations of harmonic frequencies and ultimately single-point calculations with the MP2-(SMD)/aug-cc-pVTZ level of theory.

Though we have mainly computed metal-free processes in this paper, we have also investigated related transition-metal-catalyzed processes. Truhlar and co-workers[19] have showed that optimized geometries and energies for transition-metal complexes are well predicted by M06-L in comparison to the M05-2X functional. Thus, for transition-metal processes we have optimized each intermediate using the M06-L functional with a combination of the effective core potential LANL2 along with the LANL2DZ basis set on the Ir atom and the 6-31++g(d,p) basis set on other atoms (BS1) in the gas phase and subsequently single-point solvent phase calculations have been

DOI: 10.1021/cs502129m
ACS Catal. 2015, 5, 3478−3493

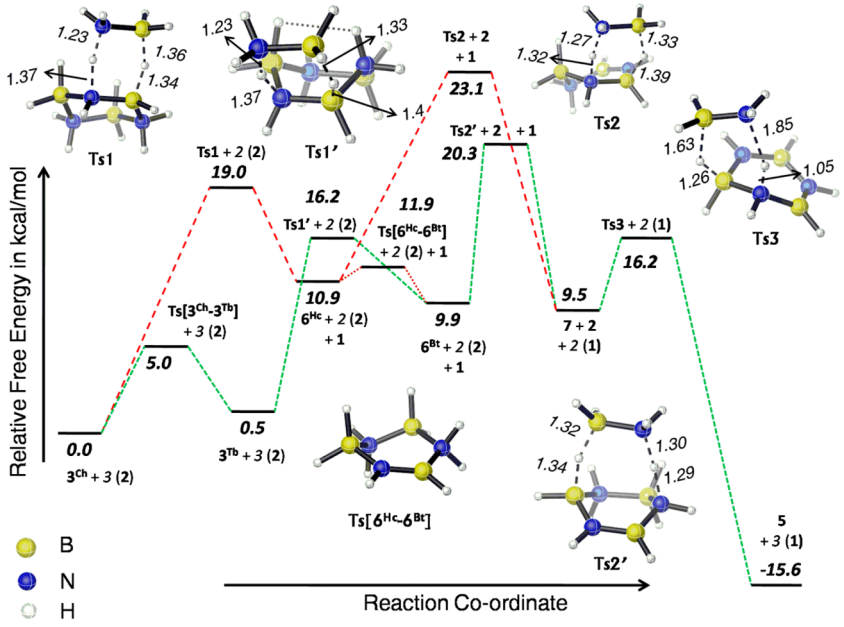

Figure 1. Free energy profile for dehydrogenation of CTB (**3**) to form borazine (**5**). Optimized geometries of important transition states are given in the figure. All bond distances shown in the figure are given in Å.

done using the same level of theory. Due to bulky ligands present in the Ir(POCOP)H_2 catalyst, we have evaluated the thermodynamic corrections obtained from harmonic frequencies on the gas phase optimized geometries (obtained by M06-L/BS1) with a combination of the effective core potential LANL2 along with the LANL2DZ basis set on the Ir atom and 6-31+g(d,p) basis set on other atoms (BS2). Solvent phase free energies were evaluated using the same method discussed previously. For comparison with the transition-metal-catalyzed process, all relevant metal-free processes were further calculated at the M06-L/BS1 level of theory. The images of the calculated structures are reported using CYLview.[20] The working equations for determining solvent phase free energy are supplied in the Supporting Information.

RESULTS AND DISCUSSION

I. Dehydrogenation of BN Cyclic Oligomers by NH_2BH_2. After release of 1 equiv of hydrogen from **1** by a type II catalyst, **2** is generated in solution, as suggested by Baker's chemical entrapment technique.[4] Our earlier theoretical endeavor has revealed the solvent-assisted reaction channels through which **2** can produce cyclic oligomers **3** and **4** with rate-determining barriers of 12.7 and 11.9 kcal/mol, respectively.[7b]

*(i). Dehydrogenation of Cyclotriborazane (CTB, **3**).* **3** is the BN analogue of cyclohexane. We have found that **3** can exist in almost two isoenergetic low-energy conformers, the chair form ($\mathbf{3}^{Ch}$) (shown in Scheme 5) and the twist-boat conformer ($\mathbf{3}^{Tb}$) (shown in Scheme 5), in contrast to its hydrocarbon analogue cyclohexane, which prefers mainly the chair conformation (see Figure 1). These findings are in agreement with the higher energy difference obtained by Findlay et al. using LCGO-MO-SCF between chair and boat conformers of cyclohexane in comparison to CTB.[21] The interconversion between these two conformers occurs through **Ts**[$\mathbf{3}^{Ch}$-$\mathbf{3}^{Tb}$] (shown in the Supporting Information), a half-chair conformer, with a free energy activation barrier of only 5.0 kcal/mol.

Natural bond orbital (NBO) charge analysis and molecular electrostatic potential (MEP) plots confirmed the protic and hydridic character of N−H and B−H bonds of $\mathbf{3}^{Ch}$ and $\mathbf{3}^{Tb}$ (see MEP and NBO charges in the Supporting Information). Therefore, it is expected that **2** can accept these bipolar hydrogens in a manner similar to that for hydrogenated boron-nitride nanotubes.[9c] **2** can pluck a proton and a hydride from $\mathbf{3}^{Ch}$ through a concerted six-membered transition state (**Ts1**) with a free energy barrier of 19.0 kcal/mol. The optimized structure of **Ts1** shows that the cyclohexane ring has a half-chair conformation (see Figure 1). After transfer of two bipolar hydrogens to **2**, $\mathbf{3}^{Ch}$ forms $\mathbf{6}^{Hc}$ (shown in Scheme 5), the half-chair conformer of the first dehydrogenated BN analogue of cyclohexane, and the transformation is endoergic by 10.9 kcal/mol. On the other hand, formation of **1** from **2** by dehydrogenation of $\mathbf{3}^{Tb}$ in a similarly concerted fashion through **Ts1′** is associated with a free energy activation barrier of 16.2 kcal/mol. The optimized structure of **Ts1′** shows that the BN analogue of cyclohexane has a boat conformation (see Figure 1). Two-hydrogen (2H) transfer as a proton and hydride from $\mathbf{3}^{Tb}$ produces $\mathbf{6}^{Bt}$ (see Scheme 5), which is more thermodynamically stable than $\mathbf{6}^{Hc}$ by 1.0 kcal/mol. The two conformers $\mathbf{6}^{Hc}$ and $\mathbf{6}^{Bt}$ can interconvert through **Ts**[$\mathbf{6}^{Hc}$-$\mathbf{6}^{Bt}$] (shown in Figure1) with a free energy barrier of 11.9 kcal/mol. Next, 2H transfer from $\mathbf{6}^{Hc}$ to another 1 equiv of **2** occurs through **Ts2** (shown in Figure 1) with a free energy barrier of 23.1 kcal/mol, whereas similar 2H transfer from $\mathbf{6}^{Bt}$ occurs through **Ts2′** (shown in Figure 1) having a free energy barrier of 20.3 kcal/mol. This difference in free energy barrier can be explained by the presence of more hydridic and protic flagpole hydrogens present in $\mathbf{6}^{Bt}$, which is confirmed by NBO analysis of $\mathbf{6}^{Hc}$ and $\mathbf{6}^{Bt}$ (see NBO charges in the Supporting Information). Both **Ts2** and **Ts2′** generate **7** (shown in Scheme 5), which lies 0.4 kcal/mol below $\mathbf{6}^{Bt}$. **7** can transfer another 1 equiv of dihydrogen to **2** to produce borazine (**5**). The free energy activation barrier for this 2H transfer is 16.2 kcal/mol, and the formation of borazine is exoergic by 15.6 kcal/mol. Overall, this mechanism of borazine formation from

DOI: 10.1021/cs502129m
ACS Catal. 2015, 5, 3478−3493

CTB has a rate-determining barrier of 20.3 kcal/mol. The rate-determining barriers turn out to be 18.0, 17.9, and 16.9 kcal/mol at the ωB97X-D, M06-2X and MP2 levels of theory, respectively. The minimum energy path for this transformation starts with a conformational change of **CTB** from chair (3^{Ch}) to twist boat (3^{Tb}), followed by three 2H transfers to in situ generated **2** (see Figure 1).

(ii). Dehydrogenation of B-(Cyclodiborazanyl)-aminoborohydride. BCDB (**4**) is another intermediate which has been identified by several groups and is thought to be a key species formed en route to borazine in dehydrogenation reactions of **1**.[6] Our NBO charge analysis studies and MEP plots suggest that NH and BH hydrogens of **BCDB** (**4**) are protic and hydridic in nature, as in **CTB** (**3**) (see MEP and NBO charges in the Supporting Information). Hence, **4** is also susceptible to dehydrogenation by **2** by concerted proton and hydride abstraction from four different locations in **4** (see Scheme 6). Free energy activation barriers for all possible

Scheme 6. All Possible Protons and Hydrides Present in 4 That Are Susceptible to Transfer to 2

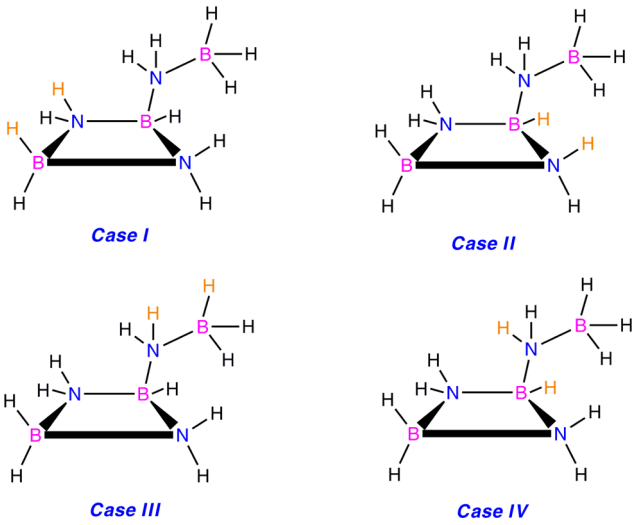

concerted dihydrogen transfers from BCDB to NH_2BH_2 and the corresponding free energy changes for product formation are shown in Table 1. Among all the possible concerted proton

Table 1. Free Energy Activation Barriers and Free Energy Changes of All Possible Dihydrogen Transfers from 4 to 2

	free energy activation barrier (kcal/mol)	free energy change of the reaction (kcal/mol)
case I	22.3	17.6
case II	26.7	23.8
case III	12.7	2.9
case IV	27.2	26.2

and hydride transfers to **2** from **4**, minimum energy dihydrogen transfer is predicted to occur from the exocyclic NH_2BH_3 unit of **4**. The free energy activation barrier for **Ts4** (shown in Figure 2) is estimated to be 12.7 kcal/mol.

After transferring the first equivalent of dihydrogen to **2**, **BCDB** forms **8** (shown in Scheme 7), which is 2.9 kcal/mol higher in free energy. **8** can undergo a ring-opening reaction to produce $NH_2{-}BH{-}NH{-}BH_2$ (**9**) (shown in Scheme 7), a BN analogue of butadiene, and **2** as suggested by McKee and co-

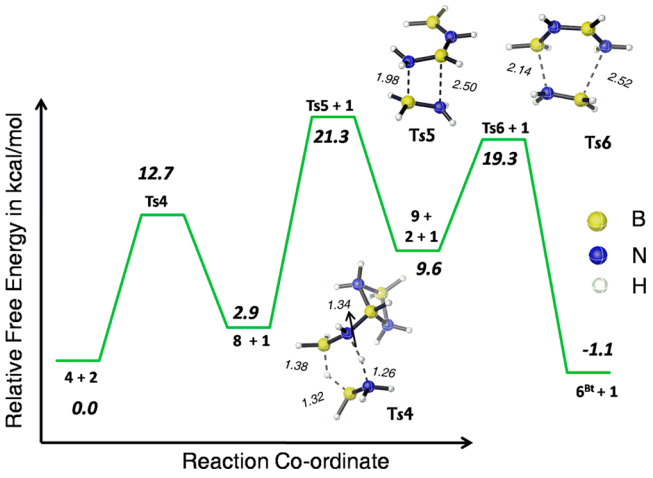

Figure 2. Free energy profile for conversion of BCDB to 6^{Bt} in the presence of **2**. Optimized geometries of important transition states are given in the figure. All bond distances shown in the figure are in Å.

Scheme 7. Formation Pathway of 6^{Bt} from 4 in the Presence of 2[a]

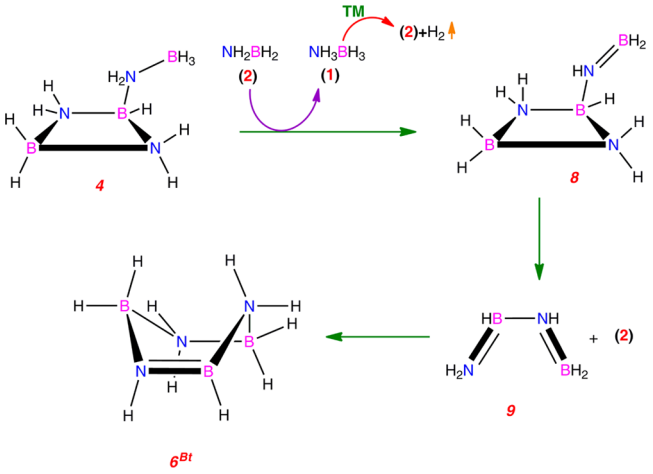

[a]TM = transition-metal-catalyzed irreversible release of H_2 from **1** and concomitant regeneration of **2**.

workers[22] through **Ts5** (shown in Figure 2) with a free energy barrier of 21.3 kcal/mol. Formation of **9** and **2** is endoergic by 9.6 kcal/mol. Not surprisingly, **9** and **2** can undergo a Diels–Alder-like reaction to produce 6^{Bt} (shown in Scheme 7). We found that the free energy barrier for this six-membered-ring formation through **Ts6** (shown in Figure 2) is 19.3 kcal/mol and formation of 6^{Bt} and **1** from **4** and **2** is exothermic by 1.1 kcal/mol. 6^{Bt} can produce borazine (**5**) through repeated dehydrogenation facilitated by **2** (as described earlier for dehydrogenation of **CTB** in Scheme 5 and Figure 1). Therefore, our theoretical investigation reveals that **4** can indeed transform to borazine (**5**) by dihydrogen removal of **2** from **4** with an overall rate-determining free energy barrier of 21.3 kcal/mol. At ωB97X-D, M06-2X, and MP2 levels of theory, the rate-determining barriers are 23.4 kcal/mol, 24.1, and 24.3 kcal/mol, respectively. The larger picture which emerges from these findings is that dehydrogenation of **3** and **4** by **2** is facile under the reported experimental conditions.

II. Formation of Polyborazylene. These findings further stoked our curiosity to seek an answer to a more challenging

DOI: 10.1021/cs502129m
ACS Catal. 2015, 5, 3478–3493

Scheme 8. Reaction Pathways for Formation of Intermediate 12, Precursor of BN Analogue of Naphthalene[a]

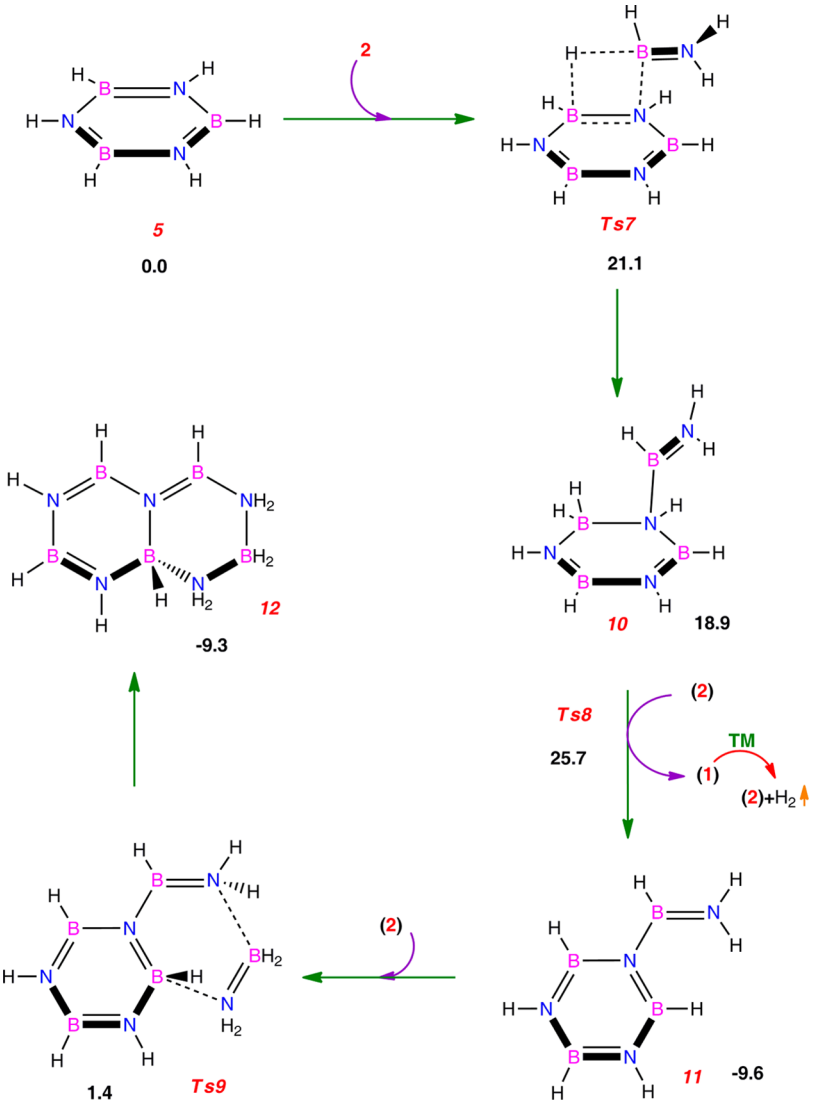

[a]The corresponding solvent phase relative energies are provided below each species. TM = transition-metal-catalyzed irreversible release of H_2 from **1** and concomitant regeneration of **2**.

question. How does a TM catalyst dehydrogenate **1** and produce polyborazylene as the end product? Our hypothesis of catalytic action of **2** would collapse if it does not explain the formation of polyborazylene in the TM-catalyzed dehydrogenation of **1**. Gratifyingly, our investigations implicate the active role of "free" **2** along with borazine in the reaction medium for yielding polyborazylene. Further dehydrogenation of borazine by **2** is not expected, as suggested by our NBO charge analysis of BH and NH hydrogens of borazine and associated MEP plots (see NBO charges and MEP in the Supporting Information).

(i). Formation of BN Analogue of Naphthalene. Unlike their carbon analogues ethylene and benzene, **2** and **5** can readily react with each other. We have found that BH of **2** can facilitate an endoergic (ΔG_{sol} = 18.9 kcal/mol) hydroboration of a BN double bond of **5** to produce **10** (shown in Scheme 8) via **Ts7** (see Figure 3). The free energy activation barrier for this hydroboration step is predicted to be 21.1 kcal/mol. As expected, **10** has distinctly protic and hydridic hydrogen atoms, which are vulnerable to dehydrogenation (see MEP and NBO

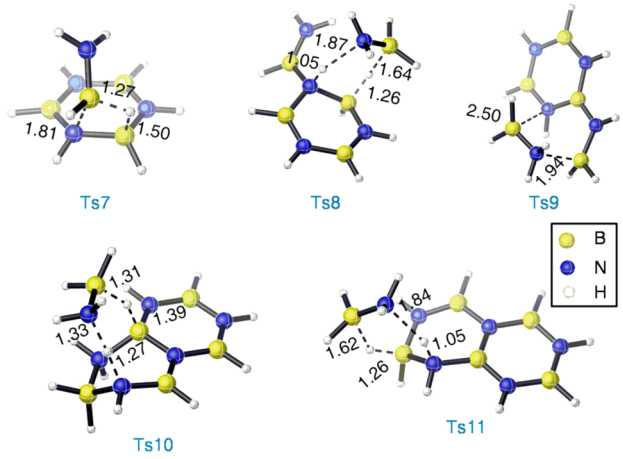

Figure 3. Optimized structures of transition states along the reaction path of polyborazylene formation from borazine (**5**). All dashed bond distances are given in Å.

DOI: 10.1021/cs502129m
ACS Catal. 2015, 5, 3478−3493

charges in the Supporting Information). **2** removes H_2 from **10** by concerted hydride and proton transfer, through **Ts8** (see Figure 3). Since **10** is relatively unstable in comparison to **5** and **2** in the free energy landscape, the overall barrier turns out to be 25.7 kcal/mol. Upon H_2 removal from **10**, the BN analogue of styrene **11** (shown in Scheme 8) is formed. The transformation of **10** to **11** is exoergic by 28.5 kcal/mol. However, a low-barrier ($\Delta G^{\ddagger}_{sol}$ = 11.0 kcal/mol) cycloaddition of **2** to **11** through **Ts9** (Figure 3) leads to the generation of intermediate **12** (Scheme 8). There are six different pairs of protons and hydrides on neighboring N and B atoms in **12** which can be transferred to **2** (see Scheme 9). We have

Scheme 9. All Distinct Protons and Hydrides of Two Neighboring N and B Atoms of 12

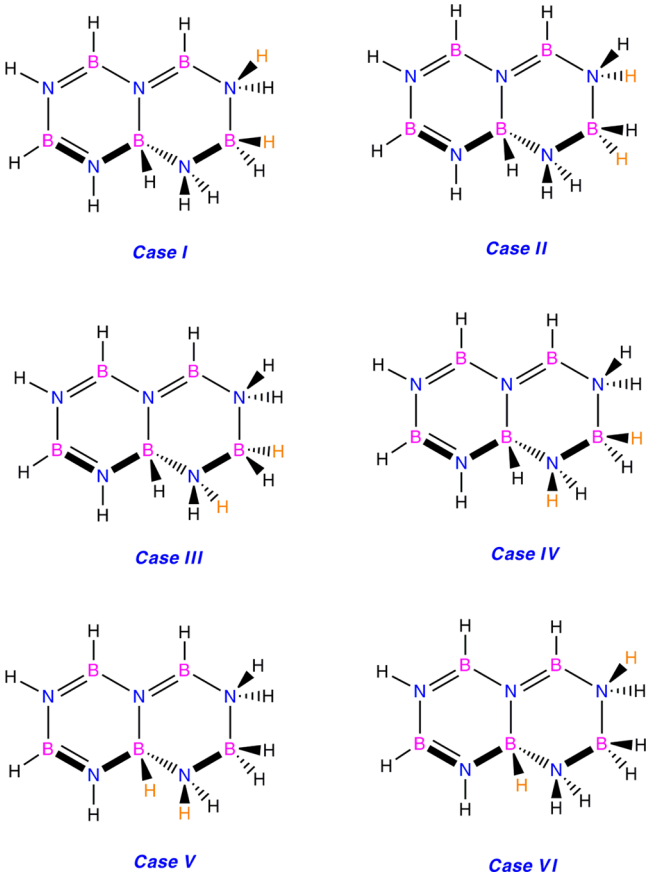

computed the free energy activation barriers and the corresponding free energy changes for product formation of each possible concerted proton and hydride transfer from **12** to **2** (shown in Table 2).

Table 2. Free Energy Activation Barriers and Free Energy Changes of All Possible Dihydrogen Transfers from 12 to 2

	free energy activation barrier (kcal/mol)	free energy change of the reaction (kcal/mol)
case I	10.1	−1.3
case II	12.2	−1.3
case III	19.8	16.7
case IV	20.8	16.7
case V	9.5	−6.3
case VI	7.6	−11.1

Among all possible concerted 2H transfers, case VI is the lowest energy pathway and also the most exothermic process. Thus, **2** initially plucks a proton and hydride from **12** through **Ts10** to form the monohydrogenated BN naphthalene unit **13** (Scheme 10). Subsequently another 2H transfer occurs from **13**

Scheme 10. Minimum Energy Pathway for Formation of Naphthalene BN Analogue 14 from 12[a]

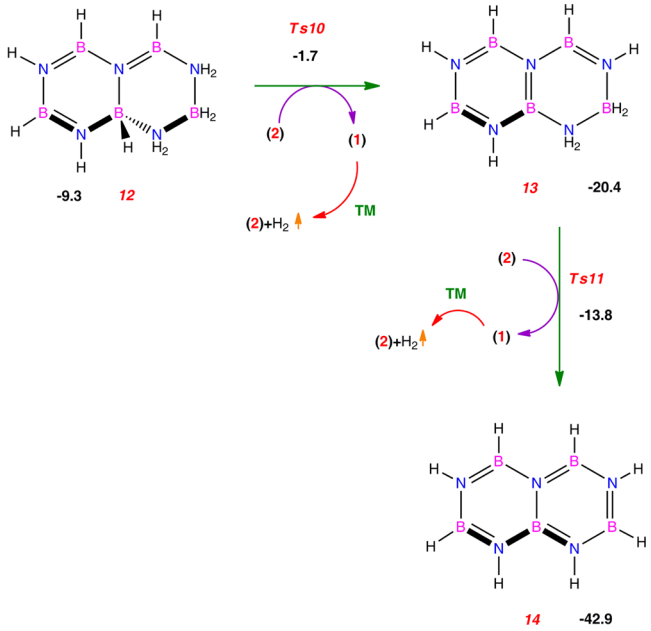

[a]TM = transition-metal-catalyzed irreversible release of H_2 from **1** and concomitant regeneration of **2**.

to **2** and produces **14**, a BN analogue of naphthalene. Free energy barriers for these two consecutive dihydrogen transfer transition states **Ts10** (Figure 3) and **Ts11** (Figure 3) are 7.6 and 6.6 kcal/mol, respectively. The transformation of **12** to **14** through this route is highly exoergic (ΔG_{sol} = −42.9 kcal/mol). The rate-determining barrier is due to **Ts8** and is estimated to be 25.7 kcal/mol. M06-2X, ωB97X-D, and MP2 levels of theory predict these free energy barrier heights as 22.5, 23.4, and 21.0 kcal/mol, respectively. One can easily see that from **14** through repeated stepwise B−H bond mediated ring formatiosn initiated by **2**, dehydrogenations triggered by **2** and cycloadditions by **2** can generate the polyborazylene framework (shown in Scheme 11).

(ii). Formation of BN Analogue of Phenathrene. The polyborazylene framework can be generated by an alternative pathway initiated through hydroboration between two borazine molecules. We have found that BH of **5** can facilitate hydroboration of a BN double bond of another **5** to produce **10′** (see Scheme 12). The free energy activation barrier for this hydroboration transition state (**Ts7′**) (shown in Scheme 12) is predicted to be 27.7 kcal/mol. Formation of the hydroborated product (**10′**) from two molecules of **5** is endoergic by 19.3 kcal/mol. Subsequently, 1 equiv of **2** can pluck BH hydride and NH proton from **10′** through **Ts8′** (see Scheme 12) with a free energy barrier of 26.3 kcal/mol. After hydride and proton transfer to **2**, **10′** produces the first cross-linked borazine unit (**11′**) (see Scheme 12), through an exoergic reaction (ΔG_{sol} = −27.4 kcal/mol). For formation of one cross-linked polyborazylene unit, the rate-determining free energy barrier is 27.7

DOI: 10.1021/cs502129m
ACS Catal. 2015, 5, 3478−3493

Scheme 11. Proposed Reaction Pathways for Formation of a Polyborazylene Framework[a]

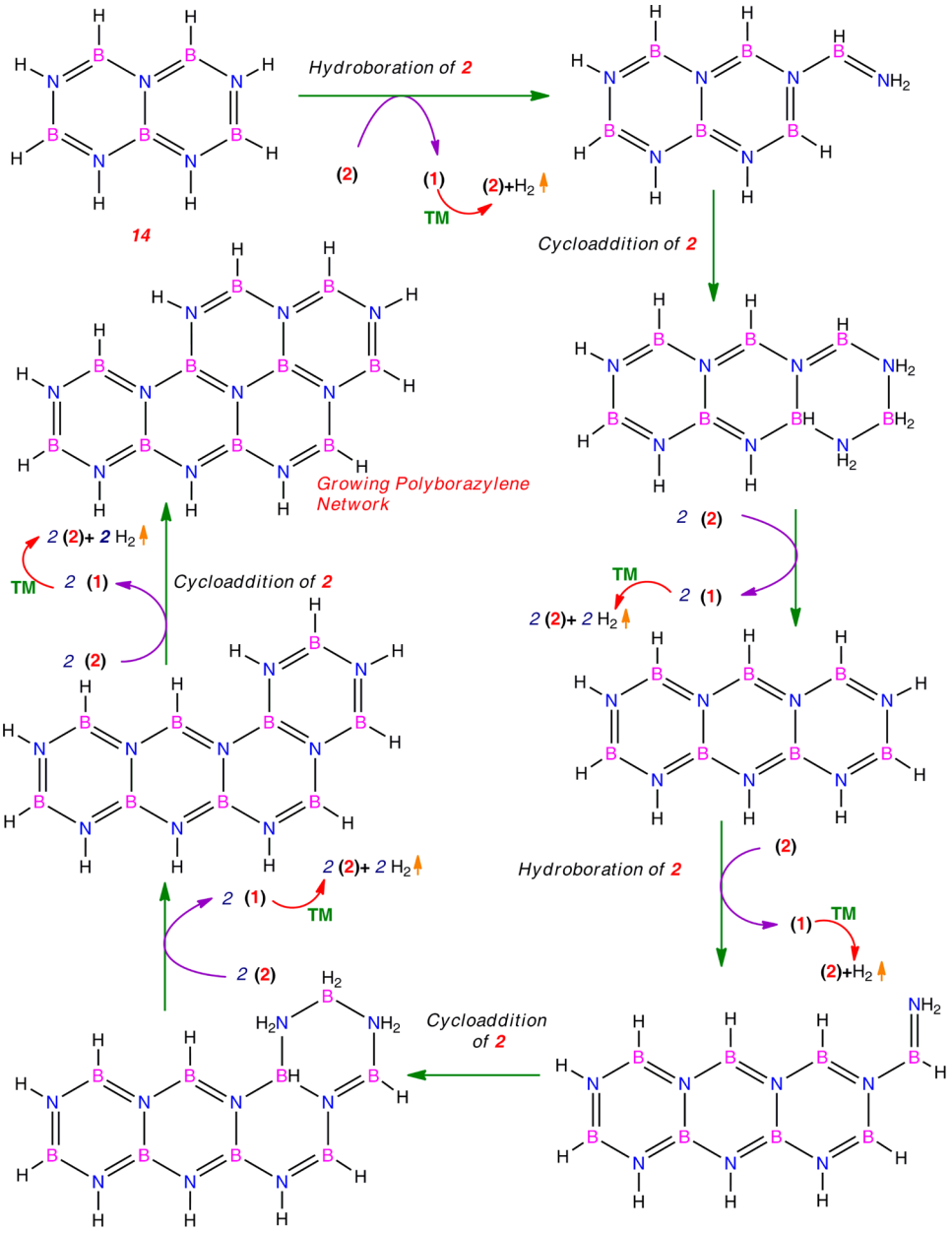

[a]TM = transition-metal-catalyzed irreversible release of H_2 from **1** and concomitant regeneration of **2**.

kcal/mol. **11′** also serves as a unit for the growth of the polyborazylene framework. **2** undergoes cycloaddition to **11′** to produce **12′** (shown in Scheme 12). **12′** has a BN framework similar to that of **12**. Thus, further dehydrogenation of **12′** will occur through dihydrogen transfers similar to those of **12**. Subsequently, two molecules of **2** dehydrogenate **12′** to produce **13′** (see Scheme 12) and **14′** (see Scheme 12), a BN analogue of phenanthrene, with an associated barrier of 12.3 kcal/mol. One can easily see that **14′** through repeated stepwise B−H bond mediated cross-linking of borazine (**5**), cycloadditions, and hydrogen removal by **2** can form the polyborazylene framework.

Our detailed theoretical analysis provides a hitherto uncharted mechanistic roadmap for polyborazylene formation (see Schemes 8, 10, 11, and 12). Initiation of polyborazylene framework formation happens through a hydroboration reaction by the B−H bond of **2** or **5** across one B−N bond of **5**. The rate-determining barrier of polyborazylene formation is due to the initial hydroboration reaction. The free energy barrier for hydroboration of **2** across **5** is predicted to be lower by 6.6 kcal/mol in comparison to hydroboration of **5** with **5**. Thus, we can conclude that polyborazylene framework formation would be initiated by the hydroboration of **2** and not by species **5**. Later the framework develops through repeated hydroborations, cycloadditions, and dehydrogenations caused by **2**. The rate-determining barrier for polyborazylene unit formation by this pathway is 25.7 kcal/mol.

III. Rate-Determining Barriers of Second and Third Equivalent Hydrogen Releases from Ammonia−Borane. In this section we have tried to find out the rate-determining step for polyborazylene formation from BN cyclic oligomers **CTB** and **BCDB** involving three broad reaction sequences:

DOI: 10.1021/cs502129m
ACS Catal. 2015, 5, 3478−3493

Scheme 12. Reaction Route for Formation of a Polyborazylene Framework Initiated through the Hydroboration of Two Borazine Units[a]

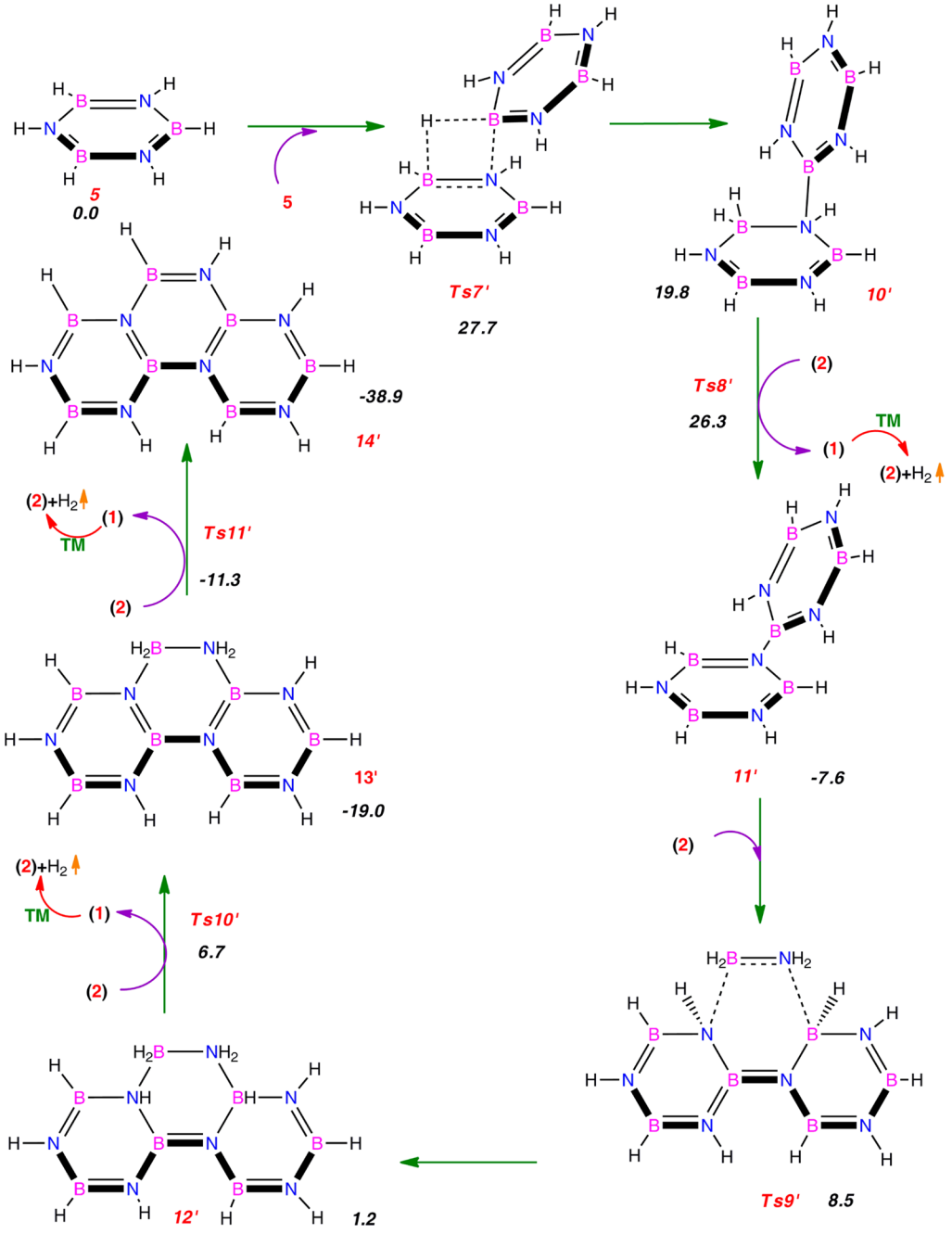

[a]TM = transition-metal-catalyzed irreversible release of H_2 from **1** and concomitant regeneration of **2**.

Table 3. Rate-Determining Barriers of the Three Consecutive Processes during Polyborazylene Formation at Different Levels of Theory

	RDB for dehydrogenation of CTB (process i, **Ts2′**), kcal/mol	RDB for dehydrogenation of BCDB (process ii, **Ts5**), kcal/mol	RDB for polyborazylene formation from **5** (process iii, **Ts8**), kcal/mol
M05-2X(SMD)/6-31++g(d,p)//M05-2X/6-31++g(d,p)	20.3	21.3	25.7
M06-2X(SMD)/6-31++g(d,p)//M06-2X/6-31++g(d,p)	17.9	24.1	22.5
M06-L(SMD)/6-31++g(d,p)//M06-L/6-31++g(d,p)	16.8	22.1	25.0
B97-D(SMD)/6-31++g(d,p)//B97-D/6-31++g(d,p)	14.3	19.5	22.5
ωB97X-D(SMD)/6-31++g(d,p)//ωB97X-D/6-31++g(d,p)	18.0	23.4	23.4
MP2(SMD)/aug-cc-pVTZ//MP2/cc-pVTZ	16.9	24.3	21.0

DOI: 10.1021/cs502129m
ACS Catal. 2015, 5, 3478−3493

(i) dehydrogenation of **CTB** by **2** to yield borazine (**5**)
(ii) dehydrogenation of **BCDB** performed by **2** to form borazine (**5**)
(iii) hydroboration, dehydrogenation, and cycloaddition triggered by **2** on borazine to form polyborazylene

Hence, one needs to compare the rate-limiting barriers from each of these processes to determine the overall rate-determining barrier for polyborazylene formation. Inconsistencies regarding the rate-determining barrier arise when we compare the barriers predicted by different functionals and the MP2 method (see Tables 3−6). We find that M05-2X, M06-L, and B97-D predict reaction sequence iii to be the rate-limiting step for polyborazylene formation, whereas MP2 and M06-2X indicates that process ii is the rate-determining process. On the other hand, ωB97X-D predicts both processes ii and iii have the highest RDB. Among the different theoretical models one may argue that post-Hartree−Fock ab initio method MP2 is the most reliable. However, MP2-predicted barriers are significantly dependent on basis sets and are very much vulnerable to basis set superposition error. We note that reaction sequence ii involves cleaving of a BN bond in a four-membered BN ring. Basis set superposition error correction can significantly affect barrier heights. Hence, we checked the crucial barriers with larger basis sets. Basis set superposition error can be eliminated through extrapolation of MP2 numbers to the complete basis set limit. Unfortunately, we were unable to conduct a complete basis set extrapolation at the MP2 level of theory due to the large number of basis functions required for the species involved. At the MP2(SMD)/aug-ccpVQZ//MP2/cc-pVTZ level of theory we find that the predicted barriers for reaction sequences ii and iii are 24.0 and 22.6 kcal/mol, respectively. This finding clearly indicates that the predicted barriers for reaction sequences ii and iii are significantly sensitive to the quality of basis sets employed in the study. In fact we find even the DFT numbers are also appreciably dependent on the choice of basis sets. For removing this apparent contradiction between different functionals, we have evaluated free energy activation barriers due to **Ts5** and **Ts8** using M05-2X, M06-2X, B97-D, M06-L, and ωB97X-D functionals with Pople's 6-311++g(d,p) basis set on each atom. All of the functionals unanimously predict that process iii is the slowest step of the whole process (see Table 5). Incidentally, M06-2X predicts the reaction sequence iii to be the rate-limiting barrier on using a triple-ζ basis set, although the difference of barrier heights between reactions ii and iii is only 0.1 kcal/mol, which is much smaller than the window of error of any DFT method. Thus, it is observed that M06-2X is the most sensitive functional among the aforementioned functionals toward basis set superposition error. Hence, we have rechecked the change in barrier heights with increasing basis set size using Dunning's family of augmented correlation consistent basis sets for M06-2X (see Table 6).

We also observe the change of barrier height with increase of basis function for M062-X, which clearly indicates that process iii is the rate-limiting sequence (see Table 6).

Although the general picture which has emerged from our study suggests that **2** acts as a transfer dehydrogenation agent to produce borazine (**5**), polyborazylene from cyclic oligomers such as **3** and **4** leads to the formation of **1** for type II catalyst (see Scheme 13). The rate-determining barrier of the whole dehydrogenation process is 25.7 kcal/mol, which stems out from the hydroboration of **2** across the B−N bond of **5**. Thus, the role of the TM catalyst may be limited to the removal of 1 equiv of H_2 from **1** to regenerate **2** to propagate dehydrogenation of the oligomers produced from **2**. Transition-metal catalysts which produce ample amounts of "free **2**" as an intermediate and do not entrap **2** through any low barrier side reaction are likely to facilitate more than 1 equiv of hydrogen removal from **1**. Our proposed mechanistic framework generally is consistent with the existing experimental knowledge in this area and can rationalize most of the observed trends. It is known that some transition-metal catalysts such as Ir(POCOP)H_2, Ru-PNP, and $[Ir(PCy_3)_2H_2]^+$ can catalyze polyaminoborane formation from units of **2**.[2a−f] Thus, this fast side reaction channel of polyaminoborane quickly consumes **2** that is formed from dehydrogenation of **1** from the reaction medium and prevents formation of the precursor oligomers of borazine, **3** and **4**, and also limits any dehydrogenation facilitated by **2**. This in turn debilitates type I catalysts from extracting more than 1 equiv of H_2 from **1**. Although Baker and co-workers[4] reported that a significant amount of borazine is obtained for Ir(POCOP)H_2-catalyzed dehydrogenation of **1** at 60 °C, they had also obtained significant trapping product with cyclohexene in the same experiment, which indicates the presence of "free NH_2BH_2" in

Table 4. Rate-Determining Barriers of the Two Consecutive Processes during Polyborazylene Formation Using Different Basis Functions for MP2

	RDB for dehydrogenation of BCDB (process ii, **Ts5**), kcal/mol	RDB for polyborazylene formation from **5** (process iii, **Ts8**), kcal/mol
MP2(SMD)/aug-cc-pVDZ//MP2/cc-pVTZ	23.2	19.8
MP2(SMD)/aug-cc-pVTZ//MP2/cc-pVTZ	24.3	21.0
MP2(SMD)/aug-cc-pVQZ//MP2/cc-pVTZ	24.0	22.6
MP2(SMD)/aug-cc-pV5Z//MP2/cc-pVTZ	24.0	−[a]

[a]Beyond computation due to huge computational cost.

Table 5. Free Energy Activation Barriers of Ts5 and Ts8 Re-Evaluated using M05-2X, M06-2X, B97X-D, M06-L, and B97-D Functionals with Valence Triple-ζ Basis Sets

	RDB for dehydrogenation of BCDB (process ii, **Ts5**), kcal/mol	RDB for polyborazylene formation from **5** (process iii, **Ts8**), kcal/mol
M05-2X(SMD)/6-311++g(d,p)//M05-2X/6-311++g(d,p)	19.7	26.5
M06-2X(SMD)/6-311++g(d,p)//M06-2X/6-311++g(d,p)	23.4	23.5
ωB97X-D(SMD)/6-311++g(d,p)//ωB97X-D/6-311++g(d,p)	22.6	24.4
M06-L(SMD)/6-311++g(d,p)//M06-L/6-311++g(d,p)	22.4	25.4
B97-D(SMD)/6-311++g(d,p)//B97-D/6-311++g(d,p)	18.7	23.4

DOI: 10.1021/cs502129m
ACS Catal. 2015, 5, 3478−3493

Table 6. Free Energy Activation Barriers of Ts5 and Ts8 Re-Evaluated using M06-2X Functional with Different Basis Functions

	RDB for dehydrogenation of BCDB (process ii, **Ts5**), kcal/mol	RDB for polyborazylene formation from **5** (process iii, **Ts8**), kcal/mol
M06-2X(SMD)/aug-cc-PVDZ//M06-2X/6-311++g(d,p)	24.6	21.1
M06-2X(SMD)/aug-cc-PVTZ//M06-2X/6-311++g(d,p)	22.8	23.5
M06-2X(SMD)/aug-cc-PVQZ//M06-2X/6-311++g(d,p)	22.9	23.7

Scheme 13. Reaction Channels Leading to Formation of Polyaminoborane for Cases of Type I Catalysts and Polyborazylene for Type II Catalysts[a]

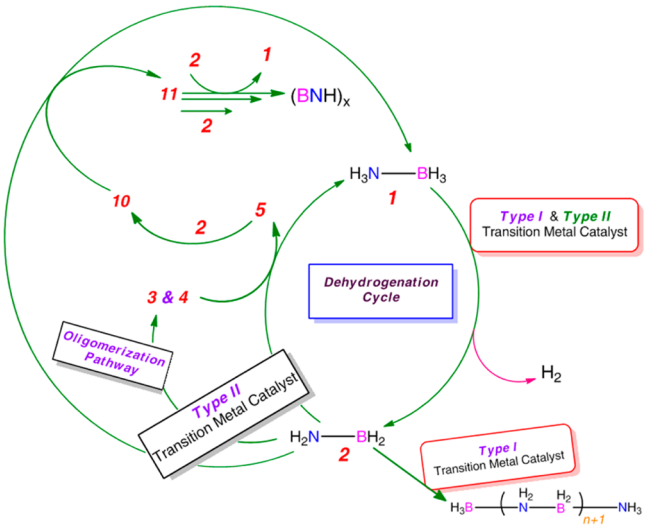

[a]The structures of **3**, **4**, **5**, **10**, and **11** are shown in earlier schemes and figures.

solution. Thus, at higher temperatures, type I catalysts may produce some borazine, as the channels which produce and dehydrogenate **3** and **4** by **2** become somewhat competitive with polyaminoborane formation. Additionally, side reactions such as catalyst deactivation by an intermediate can prevent a TM catalyst from forming polyborazylene. Williams and co-workers demonstrated that Shvo's catalyst becomes deactivated by hydroboration of borazine at the active site of the catalyst.[6c] Thus, for Shvo's catalyst hydroboration of borazine molecules by **2** does not occur, thus preventing release of more than 2 equiv of hydrogen from **1**. A comprehensive viable mechanistic picture of dehydrocoupling of ammonia–borane (**1**) by various transition-metal catalysts (both type I and type II) obtained from our theoretical study is portrayed in Scheme 13. The mechanistic scheme portrayed in Scheme 13 is applicable to homogeneous catalytic systems where the TM catalysts would dehydrogenate **CTB** and **BCDB** at higher barriers in comparison to those predicted for free NH_2BH_2. Hence, it appears that the role of TM catalysts in many cases may be limited to the first equivalent H_2 removal from **1**.

However, one may argue that TM catalysts may have a broader role in exuding greater equivalents of hydrogen from **1** in comparison to the limited role delineated here. Incidentally, most TM catalysts bear bulky ligands which are likely to prevent them from binding **3** or **4** or the growing polyborazylene framework favorably at the TM center for further dehydrogenation due to steric encumbrance. This would plausibly increase the overall dehydrogenation barrier at the TM center. To explore this angle, we have investigated first dihydrogen elimination from **3** and **4** by a bulky dehydrogenating agent (imine),[6b] N-heterocylic carbene, which was implicated by a theoretical study by Zimmerman et al.[5b] for participating in dehydrogenation of **1** for the $Ni(NHC)_2$ catalyst and an Ir-pincer transition-metal catalyst.[2a] We have compared the catalytic proficiency of these dehydrogenating agents with that of NH_2BH_2 (**2**) by comparing the respective barriers for dehydrogenation of oligomers of NH_2BH_2.

IV. Dehydrogenation of Cyclic Oligomers by Imine. Berke and co-workers[6b] reported that an imine (**Im**) can dehydrogenate ammonia–borane (**1**) to produce amine (**Am**), borazine, and polyborazylene (see Scheme 14). Their

Scheme 14. Transfer Hydrogenation of an Imine, *N*-Benzylideneaniline, by Ammonia–Borane To Produce Amine and Polyborazylene, As Reported by Berke and Co-Workers[6b]

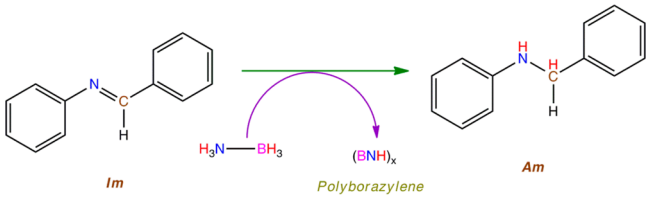

theoretical and experimental endeavor shows that imine dehydrogenates ammonia–borane through concerted proton hydride abstraction involving a six-membered transition state.[6b] We have used *N*-benzylideneaniline (**Im**) as a model dehydrogenating agent to compute the barriers for dehydrogenation of cyclic oligomers such as CTB (**3**) and BCDB (**4**) to produce borazine and to get an idea how the barriers of dehydrogenation compare with those by NH_2BH_2 (**2**). Furthermore, it would also provide us an idea of how much the barriers would increase with a more sterically demanding dehydrogenating agent. BCDB (**4**) and **Im** initially form the conjugate hydrogen-bonded intermediate $\mathbf{Im}^{\mathbf{BCDB}}$ (shown in Figure 4), which is 2.7 kcal/mol higher in free energy than the separated reactants. We have found that the free energy barrier for the transition state ($\mathbf{Ts\_Im}^{\mathbf{BCDB}}$) (shown in Figure 4) involving first dihydrogen abstraction from BCDB (**4**) is 21.6 kcal/mol, whereas NH_2BH_2 (**2**) can first pluck dihydrogen from BCDB (**4**) with a free energy barrier of 12.7 kcal/mol (see Figure 2). Following this we have investigated dehydrogenation of CTB by **Im**. Initially **Im** forms the similar hydrogen bonded intermediate $\mathbf{Im}^{\mathbf{CTB}}$ (shown in Figure 4) with CTB (**3**), where one NH proton of CTB is hydrogen bonded with the lone pair of N present in **Im** (shown in Scheme 10). Formation of $\mathbf{Im}^{\mathbf{CTB}}$ from the separated reactants is endoergic by 0.9 kcal/mol. We have found that the free energy barrier for first dihydrogen abstraction from CTB through a concerted transition state ($\mathbf{Ts\_Im}^{\mathbf{CTB}}$) (see Figure 4) is 25.3 kcal/mol. In contrast, NH_2BH_2 (**2**) can pluck two hydrogens (2H) from CTB (**3**) with a free energy barrier of 16.2 kcal/mol (see Figure 1). The predicted barrier for dehydrogenation of CTB to form borazine through dehydrogenation by imine is prohibitively high and

DOI: 10.1021/cs502129m
ACS Catal. 2015, 5, 3478–3493

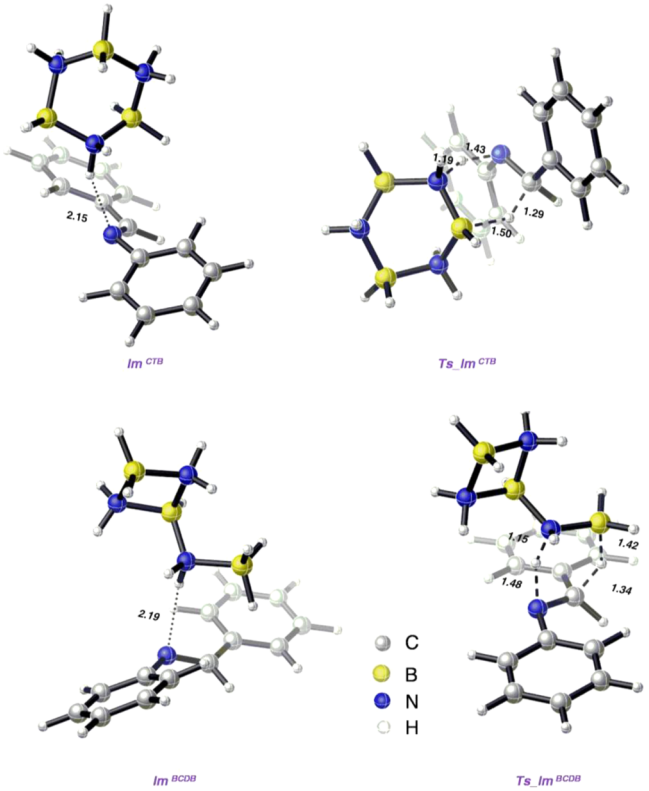

Figure 4. Optimized geometries of intermediates and transition states in the dehydrogenation of CTB and BCDB by the dehydrogenating agent *N*-benzylidineaniline (**Im**). All bond distances shown in the figure are given in Å.

would not be a significant channel for formation of the experimentally observed BN-based byproducts under the reported experimental conditions.[6b] This conclusively shows that borazine produced in this reaction is actually formed by the dehydrogenating action of NH_2BH_2 (**2**).[6b] The $NH_3{\cdot}BH_3$ (**1**) formed as a byproduct due to dehydrogenation carried out by **2** is subsequently dehydrogenated by **Im**, thus resulting in conversion of all of the imine to its hydrogenated form. Thus, our proposed transfer dehydrogenation cycle similar to that for type II transition-metal catalysts (see Scheme 13) is operative in the case of polyborazylene formation from dehydrocoupling of **1** by **Im**. Here, the dehydrocoupling agent **Im** only performs dehydrogenation of **1** to produce free **2** required for greater equivalents of hydrogen removal from **1**.

V. Dehydrogenation of Cyclic Oligomers by N-Heterocyclic Carbene. Earlier Zimmerman and co-workers have shown that free N-heterocyclic carbene (NHC) can dehydrogenate ammonia−borane to produce aminoborane.[5b] They have seen that carbene dehydrogenates ammonia−borane through a concerted transition state where simultaneous B−H and N−H bond breaking is involved.[5b] This concerted dehydrogenation step for the first equivalent of H_2 removal clearly explains the observed kinetic isotope effect, which suggests that both B−H and N−H bonds are cleaved in the rate-limiting step.[5b] Thus, this step is an important subcycle for dehydrogenation of ammonia−borane catalyzed by Ni-$(NHC)_2$.[5b] $Ni(NHC)_2$ can liberate 2.5 equiv of hydrogen from ammonia−borane.[2h] Hence, it is important to compare the free energy activation barriers for dehydrogenation of BN-cyclic oligomers by carbene to investigate if the NHC ligand generated from the decomposed catalyst has any role in extracting the second and third equivalents of hydrogen from ammonia−borane.

Zimmerman and co-workers[5b] have shown that **NHC** (see Figure 5) first forms an intermediate with ammonia−borane. After that a concerted dihydrogen transfer occurs to form aminoborane and hydrogenated NHC. Ammonia−borane initially forms a complex with **NHC**, **NHC_AB** (see Figure 5), which is 1.0 kcal/mol stable in terms of free energy. Subsequent concerted dehydrogenation of **1** by **NHC** through **TS**[**NHC_AB**] (see Figure 5) has a free energy activation barrier of 16.7 kcal/mol. We find the stabilization obtained by interaction of NHC with BCDB is 0.3 kcal/mol (for formation of **NHC_BCDB**) (see Figure 5). Dehydrogenation of the exocyclic $-NH_2-BH_3$ unit of **BCDB** through **TS**-[**NHC_BCDB**] has a free energy activation barrier of 20.2 kcal/mol. Formation of **NHC_CTB** (see Figure 5) is endothermic by 1.5 kcal/mol. The free energy barrier of concerted dihydrogen transfer to **NHC** from CTB through **Ts**[**NHC_CTB**] (see Figure 5) is 25.6 kcal/mol.

If we compare NHC-catalyzed and NH_2BH_2-catalyzed dehydrogenations of CTB and BCDB, we find

(1) dehydrogenation of BCDB by NHC has a 7.5 kcal/mol higher free energy activation barrier
(2) dehydrogenation of CTB by NHC has a 9.4 kcal/mol higher free energy activation barrier

From these results we can conclude that dehydrogenation of CTB and BCDB is favorable by NH_2BH_2 rather than the NHC itself.

VI. Dehydrogenation by Ir(POCOP)H_2 Catalyst. We have investigated the dehydrogenation barriers of BCDB (**4**) and CTB (**3**) using Ir(POCOP)H_2 to confirm that dehydrogenation of BN cyclic oligomers happens through the catalytic effect of NH_2BH_2. Though Ir(POCOP)H_2 is a type I catalyst, it behaves as a type II catalyst at 60 °C.[4] This provides the justification for investigating the Ir(POCOP)H_2-catalyzed dehydrogenation barriers for CTB (**3**) and BCDB (**4**). Additionally, several theoretical studies on this particular catalytic system by different groups have been reported and most of the facets of this catalytic system are well understood.[5a,f,g,8]

We have found that BCDB (**4**) initially forms the intermediate $\mathbf{Ir^{BCDB}}$ with Ir(POCOP)H_2, where the BH hydride of the exocyclic BH_3 end in BCDB (**4**) interacts with the Ir center. Formation of $\mathbf{Ir^{BCDB}}$ from **4** and Ir(POCOP)H_2 is endoergic by 2.7 kcal/mol. Dehydrogenation of **4** occurs through a six-membered concerted transition state ($\mathbf{Ts\_Ir^{BCDB}}$) (see Figure 6) by overcoming a free energy barrier of 20.4 kcal/mol. However, NH_2BH_2 (**2**) performs the same feat by overcoming a barrier of 11.9 kcal/mol. Similar to the case for **4**, CTB (**3**) forms the intermediate $\mathbf{Ir^{CTB}}$ with iridium catalyst, which is 2.8 kcal/mol endoergic in comparison to the two separated reactants. The six-membered concerted transition state [$\mathbf{Ts\_Ir^{CTB}}$] (see Figure 6) by which first dihydrogen is released from **3** by Ir catalyst has a 25.5 kcal/mol free energy barrier. However, **2** carries out this task by surmounting a barrier of only 15.2 kcal/mol. Thus, the distinct difference in free energy barrier *heights* suggests that **2** is better suited to facilitate the dehydrogenation of BN cyclic oligomers than the bulky transition-metal catalyst. It is noteworthy that the Ir catalyst abstracts 2H from **1** at a barrier of 15.3 kcal/mol.

Our calculation shows that a bulky transition-metal catalyst has higher free energy activation barriers in comparison to that

DOI: 10.1021/cs502129m
ACS Catal. 2015, 5, 3478−3493

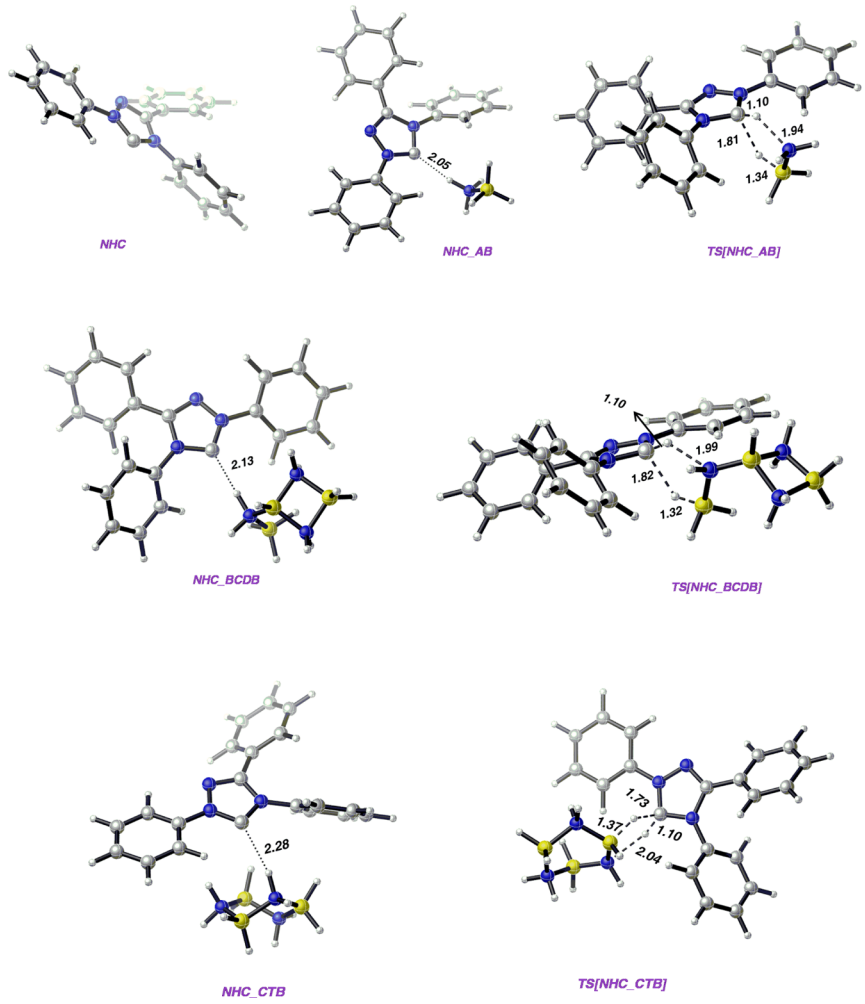

Figure 5. Optimized geometries of intermediates and transition states in the dehydrogenation of **AB**, **CTB**, and **BCDB** by the dehydrogenating agent N-heterocyclic carbene (**NHC**). All bond distances shown in the figure are given in Å. The color coding for Figure 4 has been followed here.

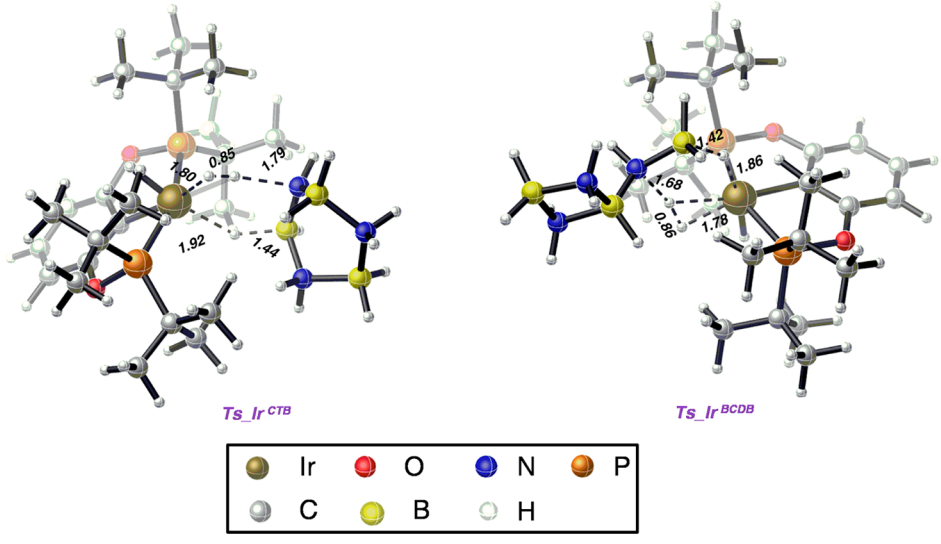

Figure 6. Optimized geometries of the respective transition states for the first dehydrogenation of CTB (**Ts_Ir**^{CTB}) and BCDB (**Ts_Ir**^{BCDB}) by Ir(POCOP)H_2 catalyst. All bond distances shown in the figure are given in Å.

for NH_2BH_2 (**2**) for dihydrogen removal from CTB (**3**) and BCDB (**4**), probably due to significant steric issues in the former case. In the particular case of the iridium catalyst we indeed find that NH_2BH_2 effectively assists in producing borazine at elevated temperatures and the role of TM catalyst is limited to removal of the first equivalent of H_2 from **1**. On

DOI: 10.1021/cs502129m
ACS Catal. 2015, 5, 3478−3493

consideration of the three specific cases that we have examined, it appears that the role of free NH_2BH_2 in the removal of more than 1 equiv of hydrogen cannot be undermined. However, on the basis of the current set of findings it would be not be prudent to totally discount the possibility of a direct participation of TM catalysts in the removal of H_2 from BCDB and CTB to form borazine. A case by case investigation is certainly needed to examine the role of TM catalyst for each catalytic system for ammonia−borane dehydrogenation. Evidently, such a case by case investigation for all of the catalytic systems is beyond the scope of the current work. The proposed mechanistic picture in Scheme 13 would change only if the barriers of dehydrogenation of BCDB, CTB, and a network of growing polyborazylene constituent fragments by the TM catalyst itself are lower than those by NH_2BH_2. Having said that, one needs to keep in mind that the binding of the growing polymeric BN sheet with a bulky transition-metal catalyst would be less favorable due to huge steric encumbrance between the bulky ligands present in the transition-metal catalyst and the BN sheet. "Free NH_2BH_2 (**2**)" in the reaction medium, however, would not face any such steric impediment in dehydrogenating the growing BN sheet due to its small size. Thus, we can infer that a bulky transition-metal catalyst does not participate directly in the removal of greater equivalents of hydrogen from **1**: i.e. it does not dehydrogenate **3**, **4**, or the growing BN sheet by itself.

CONCLUSION

From our computational studies on borazine and polyborazylene formation through transition-metal-catalyzed (type II) ammonia−borane dehydrocoupling, we may draw the following inferences.

(1) "Free NH_2BH_2" plausibly has an active role in the release of multiple equivalents of hydrogen from ammonia−borane. When NH_2BH_2 forms polyaminoborane with the help of a transition-metal catalyst framework, only 1 equiv of hydrogen is released from ammonia−borane. If the TM-catalyzed polyaminoborane formation channel is absent, NH_2BH_2 forms cyclic BN oligomers such as **CTB** and **BCDB**, which later form borazine through concerted dehydrogenation by free NH_2BH_2. We find that free NH_2BH_2 is more effective in dehydrogenating **BCDB** and **CTB** in comparison to Brookhart's Ir pincer catalyst, N-heterocyclic carbene, and imines. This possibly indicates that NH_2BH_2 has a significant role in the formation of borazine and polyborazylene complexes in most TM-catalyzed reactions.

(2) From our study it appears that the role of the transition-metal catalyst may be limited to performing the transformation of ammonia−borane to aminoborane and hydrogen. While this may be true for some cases, many more theoretical case studies are needed to establish if a TM catalyst actively participates in dehydrogenating aminoborane-based oligomers.

(3) Polyborazylene can be formed by a chain of hydroboration reactions, cycloadditions, and dehydrogenations catalyzed by "free NH_2BH_2" on borazine.

(4) An ideal transition-metal catalyst for maximum hydrogen release from ammonia−borane should not interact with in situ generated NH_2BH_2, and it should not be inhibited by borazine.

In summary, our proposed catalytic cycle explains the formation of borazine and polyborazylene upon dehydrogenation of ammonia−borane (**1**) by type II catalysts. This theoretical insight also provides key factors 1−4 for designing catalysts to release the second and third equivalents of hydrogen from ammonia−borane in order to unleash the full hydrogen storage capacity of this important material.

ASSOCIATED CONTENT

Supporting Information

The following file is available free of charge on the ACS Publications website at DOI: 10.1021/cs502129m.

Computational details, including optimized structures and coordinates of intermediates and transition states, IRC of important reaction steps, molecular electrostatic potential plots, and NBO charges of important intermediates (PDF)

AUTHOR INFORMATION

Corresponding Author

*E-mail for A.P.: rcap@iacs.res.in.

Funding

S.B. thanks the CSIR of India for a research fellowship. A.P. thanks the DST of India for providing financial support through the "Fast track" project (No. SR/FT/CS-118/2011).

Notes

The authors declare no competing financial interest.

REFERENCES

(1) (a) Marder, T. B. *Angew. Chem., Int. Ed.* **2007**, *46*, 8116−8118. (b) Hamilton, C. W.; Baker, R. T.; Staubitz, A.; Manners, I. *Chem. Soc. Rev.* **2009**, *38*, 279−293. (c) Staubitz, A.; Robertson, A. P. M.; Manners, I. *Chem. Rev.* **2010**, *110*, 4079−4124. (d) Leitao, E. M.; Jurca, T.; Manners, I. *Nat. Chem.* **2013**, *5*, 817−829.

(2) (a) Denney, M. C.; Pons, V.; Hebden, T. J.; Heinekey, D. M.; Goldberg, K. I. *J. Am. Chem. Soc.* **2006**, *128*, 12048−12049. (b) Staubitz, A.; Presa Soto, A.; Manners, I. *Angew. Chem., Int. Ed.* **2008**, *47*, 6212−6215. (c) Staubitz, A.; Sloan, M. E.; Robertson, A.; Friedrich, A.; Schneider, S.; Gates, P. J.; Schmedt auf der Günne, J.; Manners, I. *J. Am. Chem. Soc.* **2010**, *132*, 13332−13345. (d) Blaquiere, N.; Diallo-Garcia, S.; Gorelsky, S. I.; Black, D. A.; Fagnou, K. *J. Am. Chem. Soc.* **2008**, *130*, 14034−14035. (e) Marziale, A. N.; Friedrich, A.; Klopsch, I.; Drees, M.; Celinski, V. R.; Schmedt auf der Günne, J.; Schneider, S. *J. Am. Chem. Soc.* **2013**, *135*, 13342−13355. (f) Kumar, A.; Johnson, H. C.; Hooper, T. N.; Weller, A. S.; Algarra, A. G.; Macgregor, S. A. *Chem. Sci.* **2014**, *5*, 2546−2553. (g) Esteruelas, M. A.; Lopez, A. M.; Mora, M.; Oñate, E. *ACS Catal.* **2015**, *5*, 187−191. (h) Keaton, R. J.; Blacquiere, J. M.; Baker, R. T. *J. Am. Chem. Soc.* **2007**, *129*, 1844−1845. (i) Conley, B. L.; Williams, T. J. *Chem. Commun.* **2010**, *46*, 4815−4817. (j) Conley, B. L.; Guess, D.; Williams, T. J. *J. Am. Chem. Soc.* **2011**, *133*, 14212−14215. (k) Bhattacharya, P.; Krause, J. A.; Guan, H. *J. Am. Chem. Soc.* **2014**, *136*, 11153−11161. (l) Baker, R. T.; Gordon, J. C.; Hamilton, C. W.; Henson, N. J.; Lin, P.-H.; Maguire, S.; Murugesu, M.; Scott, B. L.; Smythe, N. C. *J. Am. Chem. Soc.* **2012**, *134*, 5598−5609. (m) Buss, J. A.; Edouard, G. A.; Cheng, C.; Shi, J.; Agapie, T. *J. Am. Chem. Soc.* **2014**, *136*, 11272−11275. (n) Kim, S.-K.; Han, W.-S.; Kim, T.-J.; Kim, T.-Y.; Nam, S. W.; Mitoraj, M.; Piekoś, Ł.; Michalak, A.; Hwang, S.-J.; Kang, S. O. *J. Am. Chem. Soc.* **2010**, *132*, 9954−9955. (o) Vance, J. R.; Robertson, A. P. M.; Lee, K.; Manners, I. *Chem. - Eur. J.* **2011**, *17*, 4099−4103. (p) Rossin, A.; Bottari, G.; Lozano-Vila, A. M.; Paneque, M.; Peruzzini, M.; Rossia, A.; Zanobini, F. *Dalton Trans.* **2013**, *42*, 3533−3541. (q) Rossin, A.; Rossi, A.; Peruzzini, M.; Zanobini, F. *ChemPlusChem* **2014**, *79*, 1316−1325. (r) Tang, Z.; Chen, X.; Chen, H.; Wu, L.; Yu, X. *Angew. Chem., Int. Ed.* **2013**, *52*, 5832−5835. (s) Tang, Z.; Chen, H.; Chen, X.; Wu, L.; Yu, X. *J. Am. Chem. Soc.* **2012**, *134*, 5464−5467. (t) Sonnenberg, J. F.; Morris, R. H. *ACS Catal.* **2013**, *3*, 1092−1102. (u) Metin, Ö; Mazumder, V.; Özkar, S.; Sun, S. *J. Am. Chem. Soc.* **2010**, *132*, 1468−1469. (v) Yan, J.-M.; Zhang, X.-B.; Han, S.; Shioyama, H.; Xu, Q. *Angew. Chem., Int. Ed.* **2008**, *47*, 2287−2289.

DOI: 10.1021/cs502129m
ACS Catal. 2015, 5, 3478−3493

(w) Chandra, M.; Xu, Q. *J. Power Sources* **2006**, *156*, 190−194. (x) Yao, Q.; Lu, Z.-H.; Zhang, Z.; Chen, X.; Lan, Y. *Sci. Rep.* **2014**, *4*, 7597−7604.
(3) (a) Solan, M. E.; Staubitz, A.; Clark, T. J.; Russell, C. A.; Lloyd-Jones, G. C.; Manners, I. *J. Am. Chem. Soc.* **2010**, *132*, 3831−3841. (b) Sewell, L. J.; Lloyd-Jones, G. C.; Weller, A. S. *J. Am. Chem. Soc.* **2012**, *134*, 3598−3610. (c) Rosello-Merino, M.; Lopez-Serrano, J.; Conejero, S. *J. Am. Chem. Soc.* **2013**, *135*, 10910−10913. (d) Vance, J. R.; Schafer, A.; Robertson, A. P. M.; Lee, K.; Turner, J.; Whittell, G. R.; Manners, I. *J. Am. Chem. Soc.* **2014**, *136*, 3048−3064. (e) Helten, H.; Dutta, B.; Vance, J. R.; Sloan, M. E.; Haddow, M. F.; Sproules, S.; Collison, D.; Whittell, G. R.; Lloyd-Jones, G. C.; Manners, I. *Angew. Chem.* **2013**, *125*, 455−458. (f) Chen, Y.; Fulton, J. L.; Linehan, J. C.; Autrey, T. *J. Am. Chem. Soc.* **2005**, *127*, 3254−3255. (g) Clark, T. J.; Russell, C. A.; Manners, I. *J. Am. Chem. Soc.* **2006**, *128*, 9582−9583.
(4) Pons, V.; Baker, R. T.; Szymczak, N. K.; Heldebrant, D. J.; Linehan, J. C.; Matus, M. H.; Grant, D. J.; Dixon, D. A. *Chem. Commun.* **2008**, 6597−6599.
(5) (a) Paul, A.; Musgrave, C. B. *Angew. Chem., Int. Ed.* **2007**, *46*, 8153−8156. (b) Zimmerman, P. M.; Paul, A.; Zhang, Z.; Musgrave, C. B. *Angew. Chem., Int. Ed.* **2009**, *48*, 2201−2205. (c) Yang, X.; Hall, M. B. *J. Am. Chem. Soc.* **2008**, *130*, 1798−1799. (d) Zimmerman, P. M.; Paul, A.; Musgrave, C. B. *Inorg. Chem.* **2009**, *48*, 5418−5433. (e) Butera, V.; Russo, N.; Sicilia, E. *ACS Catal.* **2014**, *4*, 1104−1113. (f) Ghatak, K.; Vanka, K. *Comput. Theor. Chem.* **2012**, *992*, 18−29. (g) Ghatak, K.; Mane, M.; Vanka, K. *ACS Catal.* **2013**, *3*, 920−927.
(6) (a) Jaska, C. A.; Temple, K.; Lough, A. J.; Manners, I. *J. Am. Chem. Soc.* **2003**, *125*, 9424−9425. (b) Yang, X.; Zhao, L.; Fox, T.; Wang, Z.-X.; Berke, H. *Angew. Chem., Int. Ed.* **2010**, *49*, 2058−2062. (c) Lu, Z.; Conley, B. L.; Williams, T. J. *Organometallics* **2012**, *31*, 6705−6714. (d) Shaw, W. J.; Linehan, J. C.; Szymczak, N. K.; Heldebrant, D. J.; Yonker, C.; Camaioni, D. M.; Baker, R. T.; Autrey, T. *Angew. Chem., Int. Ed.* **2008**, *47*, 7493−7496.
(7) (a) Zimmerman, P. M.; Paul, A.; Zhang, Z.; Musgrave, C. B. *Inorg. Chem.* **2009**, *48*, 1069−1081. (b) Malakar, T.; Roy, L.; Paul, A. *Chem. - Eur. J.* **2013**, *19*, 5812−5817. (c) Zimmerman, P. M. *Mol. Simul.* **2015**, *41*, 43−54.
(8) Bhunya, S.; Malakar, T.; Paul, A. *Chem. Commun.* **2014**, *50*, 5919−5922.
(9) (a) Robertson, A. P. M.; Leitao, E. M.; Manners, I. *J. Am. Chem. Soc.* **2011**, *133*, 19322−19325. (b) Leitao, E. M.; Stubbs, N. E.; Robertson, A.; Helten, H.; Cox, R. J.; Lloyd-Jones, G. C.; Manners, I. *J. Am. Chem. Soc.* **2012**, *134*, 16805−16816. (c) Roy, L.; Mittal, S.; Paul, A. *Angew. Chem., Int. Ed.* **2012**, *51*, 4152−4156.
(10) Frisch, M. J.; Trucks, G. W.; Schlegel, H. B.; Scuseria, G. E.; Robb, M. A.; Cheeseman, J. R.; Scalmani, G.; Barone, V.; Mennucci, B.; Petersson, G. A.; Nakatsuji, H.; Caricato, M.; Li, X.; Hratchian, H. P.; Izmaylov, A. F.; Bloino, J.; Zheng, G.; Sonnenberg, J. L.; Hada, M.; Ehara, M.; Toyota, K.; Fukuda, R.; Hasegawa, J.; Ishida, M.; Nakajima, T.; Honda, Y.;Kitao, O.; Nakai, H.; Vreven, T.; Montgomery, J. A., Jr.; Peralta, J. E.; Ogliaro, F.; Bearpark, M.; Heyd, J. J.; Brothers, E.; Kudin, K. N.; Staroverov, V. N.; Kobayashi, R.; Normand, J.; Raghavachari, K.; Rendell, A.; Burant, J. C.; Iyengar, S. S.; Tomasi, J.; Cossi, M.; Rega, N.; Millam, J. M.; Klene, M.; Knox, J. E.; Cross, J. B.; Bakken, V.; Adamo, C.; Jaramillo, J.; Gomperts, R.; Stratmann, R. E.; Yazyev, O.; Austin, A. J.; Cammi, R.; Pomelli, C.; Ochterski, J. W.; Martin, R. L.; Morokuma, K.; Zakrzewski, V. G.; Voth, G. A.; Salvador, P.; Dannenberg, J. J.; Dapprich, S.; Daniels, A. D.; Farkas, O.; Foresman, J. B.; Ortiz, J. V.; Cioslowski, J.; Fox, D. J. *Gaussian 09, Revision A.02*; Gaussian, Inc., Pittsburgh, PA, 2009.
(11) Zhao, Y.; Schultz, N. E.; Truhlar, D. G. *J. Chem. Theory Comput.* **2006**, *2*, 364−382.
(12) Marenich, A. V.; Cramer, C. J.; Truhlar, D. G. *J. Phys. Chem. B* **2009**, *113*, 6378−6396.
(13) (a) Wertz, D. H. *J. Am. Chem. Soc.* **1980**, *102*, 5316−5322. (b) Li, H.; Wang, X.; Huang, F.; Lu, G.; Jiang, J.; Wang, Z.-X. *Organometallics* **2011**, *30*, 5233−5247. (c) Yu, Z.-X.; Houk, K. N. *J. Am. Chem. Soc.* **2003**, *125*, 13825−13830. (d) Li, H.; Wang, X.; Wen, M.; Wang, Z.-X. *Eur. J. Inorg. Chem.* **2012**, 5011−5020. (e) Li, H.; Wen, M.; Wang, Z.-X. *Inorg. Chem.* **2012**, *51*, 5716−5727. (f) Zhao, L.; Huang, F.; Lu, G.; Wang, Z.-X.; Schleyer, P. v. R. *J. Am. Chem. Soc.* **2012**, *134*, 8856−8868. (g) Qu, S.; Dang, Y.; Song, C.; Wen, M.; Huang, K.-W.; Wang, Z.-X. *J. Am. Chem. Soc.* **2014**, *136*, 4974−499. (h) Ding, L.; Ishida, N.; Murakami, M.; Morokuma, K. *J. Am. Chem. Soc.* **2014**, *136*, 169−178.
(14) Zhao, Y.; Truhlar, D. G. *Theor. Chem. Acc.* **2008**, *120*, 215−241.
(15) Chai, J. D.; Head-Gordon, M. *Phys. Chem. Chem. Phys.* **2008**, *10*, 6615−6620.
(16) Zhao, Y.; Truhlar, D. G. *J. Chem. Phys.* **2006**, *125* (194101), 1−18.
(17) Grimme, S. *J. Comput. Chem.* **2006**, *27*, 1787−99.
(18) Head-Gordon, M.; Pople, J. A.; Frisch, M. J. *Chem. Phys. Lett.* **1988**, *153*, 503−06.
(19) Zhao, Y.; Truhlar, D. G. *Acc. Chem. Res.* **2008**, *41*, 157−167.
(20) Legault, C. Y. *CYLView, 1.0b*; Université de Sherbrooke, Montreal, Québec, Canada, 2009; http://www.cylview.org.
(21) Findlay, R. H. *J. Chem. Soc., Chem. Commun.* **1975**, 98−99.
(22) Nutt, W. R.; McKee, M. L. *Inorg. Chem.* **2007**, *46*, 7633−7645.

DOI: 10.1021/cs502129m
ACS Catal. 2015, 5, 3478−3493